# Fast Guest Exchange of a 1:1 Zinc Porphyrin–Amine Host–Guest Complex via a Six-Coordinated Zinc Porphyrin

**Yutaka Hitomi,*[1] Junya Ohyama,[2] Minori Takegoshi,[2] Akira Ando,[2] Takuzo Funabiki,[1] Masahito Kodera,[1] and Tsunehiro Tanaka[2]**

[1]Department of Molecular Chemistry and Biochemistry, Faculty of Science and Engineering, Doshisha University, Kyotanabe, Kyoto 610-0321

[2]Department of Molecular Engineering, Graduate School of Engineering, Kyoto University, Kyoto Daigaku Katsura, Nishikyo-ku, Kyoto 606-8501

Received January 13, 2010
E-mail: yhitomi@mail.doshisha.ac.jp

A novel zinc porphyrin receptor has been synthesized that has two identical binding pockets surrounded by six phenyl rings on both sides of the porphyrin plane. The binding of amine guests to the zinc porphyrin receptor was studied by UV–vis titration experiments. Among the amine guests, 1,4-diazabicyclo[2.2.2]octane (DABCO) showed the highest binding affinity ($\Delta G = -36.6\,\mathrm{kJ\,mol^{-1}}$ at 298 K in toluene) thanks to close contacts of DABCO with the aromatic walls of the binding pocket. The binding of DABCO was further investigated by dynamic NMR experiments. DABCO was tightly bound in one binding pocket when less than 1 equivalent of DABCO was added, but it started a rapid exchange between the two binding pockets when exceeding 1 equivalent.

Porphyrins have been frequently employed as a synthetic host in host–guest chemistry due to its rich photophysical properties and well-established synthetic routes.[1] In particular, amine coordination to zinc porphyrin has been widely utilized as a major driving force to capture small molecules in various host–guest systems,[2] and also as an organizing tool in supramolecular porphyrin assemblies such as molecular squares, boxes, circles, and coordination polymers.[3] In spite of the important roles of amine coordination to zinc porphyrins, studies on its dynamic aspects are limited.[4] Understanding host–guest systems and more complex supramolecular systems in terms of not only static, but also dynamic perspectives would provide valuable insights into the design of more stable and/or more dynamic supramolecular systems. Herein, we report a unique dynamic aspect of amine coordination to a novel zinc porphyrin **Zn-1**, in which a tightly bound amine guest is released by coordination of a second amine guest from the opposite face.

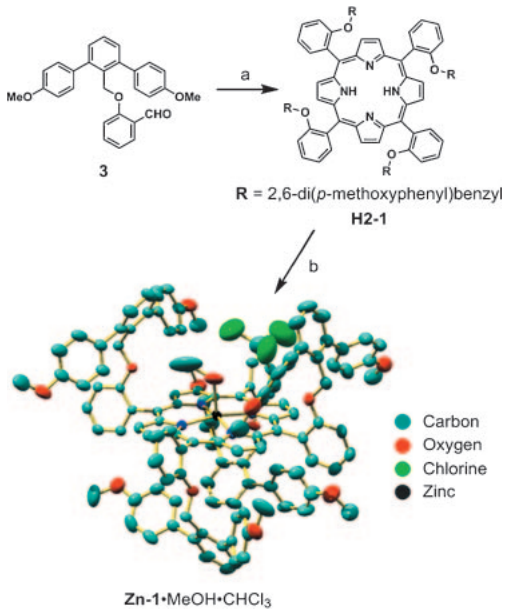


**Figure 1.** Synthetic scheme and crystal structure of **Zn-1**. a) 1) Pyrrole, $BF_3 \cdot Et_2O$, EtOH, $CHCl_3$, 2) DDQ, and 3) silica gel chromatography. b) $Zn(OAc)_2$, MeOH, $CHCl_3$.

The receptor **Zn-1** was synthesized by the condensation of pyrrole with benzaldehyde **3**.[5] Due to the sterically demanding substituents, the desired $\alpha\beta\alpha\beta$-atropisomer was preferentially obtained ($\alpha\beta\alpha\beta$:$\alpha\alpha\beta\beta$:$\alpha\alpha\alpha\beta$:$\alpha\alpha\alpha\alpha$ = 55:27:18:0)[6,7] and easily separated from the other isomers by silica gel chromatography (Figure 1). As designed, the solid structure of **Zn-1** shows two pockets surrounded by six phenyl rings on both sides of the porphyrin plane, in which one pocket accommodates one methanol and one chloroform, while the other pocket is occupied with the aromatic rings of another crystallographically identical **Zn-1** (Figure S1).[8] Furthermore, ROE (rotating frame NOE) measurements support the fact that the two equivalent pockets exist in solution (Figure S2). In order to understand the effect of the created pockets, titration of small amine guests with **Zn-1** was followed by UV–visible absorption spectroscopy (Figure S3). A nonlinear least-square analysis of the spectral changes showed a simple 1:1 complexation in all cases. The estimated binding energies are listed in Table 1, together with those for the zinc–tetraphenylporphyrin (**ZnTPP**) as a reference. Among the amine guests, 1,4-diazabicyclo[2.2.2]octane (DABCO) shows a preference for **Zn-1** over **ZnTPP** by $5.3\,\mathrm{kJ\,mol^{-1}}$. A molecular modeling study indicated that the bound DABCO closely contacts the aromatic walls of the pocket (Figure S4), which accounts for the tight binding of DABCO to **Zn-1**.

To investigate the dynamic aspects of the DABCO binding, the titration of DABCO with **Zn-1** was further investigated by $^1$H NMR spectroscopy (Figures 2 and S5). Upon the binding of DABCO to **Zn-1**, two diagnostic signals, A and B, are observed for the methylene protons of the bound DABCO ($\Delta\delta A = -3.22$, $\Delta\delta B = -5.90$), caused by the shielding effects of the porphyrin plane and phenyl groups. The two sets of signals do not shift during the titration of DABCO up to ca. 0.9 equiv, indicating that the DABCO–**Zn-1** complex is kinetically stable on the NMR time scale. Two sets of singlets (C and D)

Published on the web July 24, 2010; doi:10.1246/bcsj.20100007

**Table 1.** Binding Constants $K$ ($M^{-1}$) and the Energies $\Delta G$ ($kJ\,mol^{-1}$) for the Complexation of the Amine Guests to **Zn-1** or **ZnTPP** in Toluene at 298 K

| Host | Guest | $K$ | $\Delta G^{a)}$ | $\Delta\Delta G^{b)}$ |
|---|---|---|---|---|
| **Zn-1** | Pyridine | $5.6 \times 10^4$ | −21.3 | −0.6 |
| **ZnTPP** | Pyridine | $4.3 \times 10^4$ | −20.7 | |
| **Zn-1** | 4-Picoline | $1.9 \times 10^4$ | −24.4 | −1.5 |
| **ZnTPP** | 4-Picoline | $1.0 \times 10^4$ | −22.9 | |
| **Zn-1** | 1-Methylimidazole | $2.1 \times 10^4$ | −24.6 | 2.6 |
| **ZnTPP** | 1-Methylimidazole | $6.0 \times 10^4$ | −27.2 | |
| **Zn-1** | DABCO | $2.6 \times 10^6$ | −36.6 | −5.3 |
| **ZnTPP** | DABCO | $3.0 \times 10^5$ | −31.3 | |

a) Estimated errors within 5%. b) $\Delta\Delta G = \Delta G$(**Zn-1**) − $\Delta G$(**ZnTPP**).

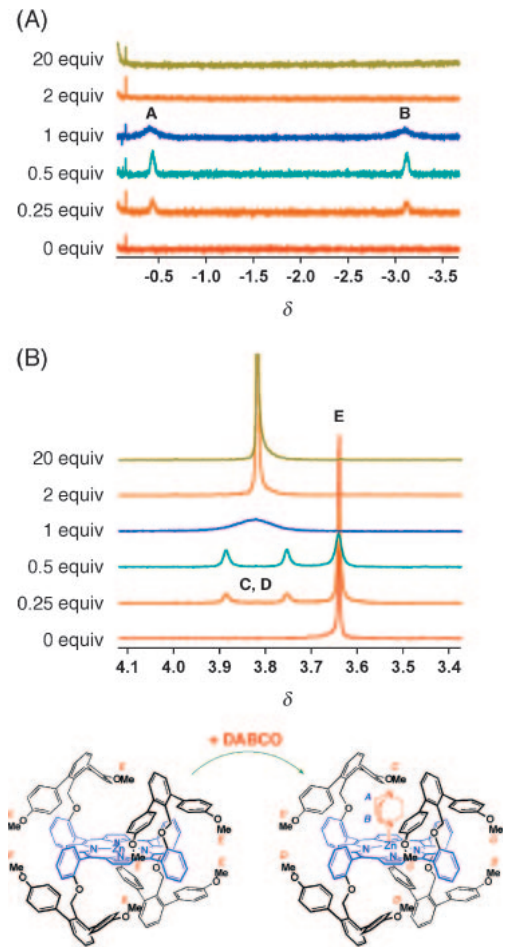


**Figure 2.** $^1$H NMR spectra from a titration experiment with the equivalents of added DABCO indicated on the left of the spectra. The labels correspond to those in the molecular models shown below.

also appear close to the singlet signal (E) of eight methoxy groups of **Zn-1**. The signals C and D are assignable to the methoxy groups on the DABCO-bound and DABCO-free sides, respectively. Upon successive addition of DABCO beyond 1 equiv, the DABCO methylene signals broaden and then disappear, while signals C and D coalesce to give a sharp singlet signal. The former phenomenon indicates the fast

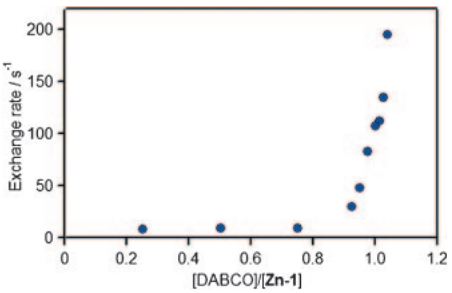


**Figure 3.** Chemical exchange rates of signals C and D with various concentrations of DABCO.

exchange of the bound DABCO with the free DABCO, and the latter shows that the two pockets of the 1:1 DABCO–**Zn-1** complex became indistinguishable on the NMR time scale.

Thus, the two pockets of the 1:1 DABCO–**Zn-1** complex are distinguishable at first and then become indistinguishable beyond 1 equiv of DABCO added. This unique behavior has never been reported in host–guest chemistry utilizing zinc porphyrin receptors to our best knowledge. This observation means that DABCO must stay in one pocket longer than the NMR time scale until the ratio of DABCO/**Zn-1** reach one; that is, the chemical exchange between species A and B shown in Scheme S1 is slow in terms of the NMR time scale, due to slow dissociation rate of DABCO from **Zn-1**, and the equilibrium between species A and B becomes fast beyond 1 equiv of DABCO added. Dynamic NMR study provided more information about the chemical exchange between species A and B. The chemical exchange rates of signals C and D are effectively constant (ca. $9\,s^{-1}$) at first and then dramatically increase when the ratio of DABCO/**Zn-1** exceeds ca. one (Figure 3). The rising curve of the chemical exchange rate suggested the involvement of unbound DABCO in accelerating the chemical exchange between species A and B, because the concentration of unbound DABCO also increases in a similar way, see Figure S6. Therefore, we concluded that unbound DABCO facilitates the chemical exchange between species A and B via a 2:1 DABCO–**Zn-1** intermediate or transition state, that is, a second DABCO occupies the unbound pocket and facilitates the dissociation of the first DABCO ligand. One may imagine that occupation of a second DABCO in the unbound pocket of the 1:1 DABCO–**Zn-1** complex deforms the porphyrin plane and/or the pockets to facilitate the dissociation of the first DABCO without forming six-coordinated **Zn-1** species, since six-coordinated zinc porphyrin complexes have never been reported in solution. However, the above-mentioned structural communication between the two pockets is highly unlikely judged from the crystal structure of **Zn-1** as well as the optimized structure of the 1:1 DABCO–**Zn-1** complex. Therefore, we propose that the associative chemical exchange proceeds via a six-coordinated transition state of **Zn-1**. Six-coordinated zinc porphyrin complexes can be seen in crystal structures,[9] and therefore, the formation of six-coordinated 2:1 DABCO–**Zn-1** species could be possible under certain conditions, especially as a transition state. In fact, we have never detected the binding of a second DABCO by NMR and UV–vis absorption spectroscopies. Moreover, our theoretical calculations support that the six-coordinated **Zn-1** species exists as a

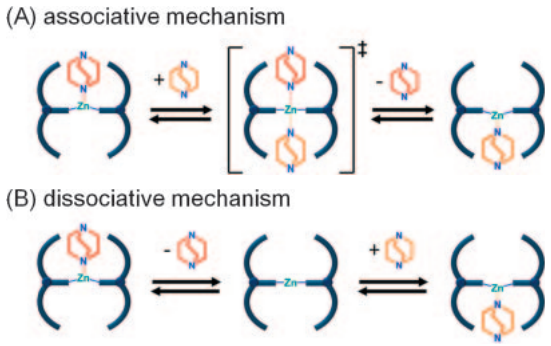


**Scheme 1.** Associative and dissociative mechanisms for DABCO exchange between the two pockets of **Zn-1**.

transition state, but not as an intermediate (Figure S7). The six-coordinated transition state of **Zn-1** has a flat porphyrin plane.

In the association mechanism, the bound DABCO dissociates from the zinc center in synchronization with the binding of an unbound DABCO to the DABCO–**Zn-1** complex (Scheme 1), and the chemical exchange rate is proportional to the concentration of unbound DABCO. This associative process is also in agreement with observed negative activation entropies for the chemical exchange of signals C and D in the presence of more than 1 equiv of DABCO (Table S1). In addition to the associative mechanism, a dissociative guest exchange process should be operative, although this process should be slower than the associative guest exchange in the host–guest system studied here. In the dissociative mechanism, the bound DABCO dissociates form the zinc center of the 1:1 DABCO–**Zn-1** complex to form a guest-free **Zn-1** and then an unbound DABCO binds in the another pocket of the guest-free Zn-1 (Scheme 1). Thus, this process involves the formation of guest-free **Zn-1** by the dissociation of DABCO from the zinc center of the 1:1 DABCO–**Zn-1** complex. Therefore, the exchange rate must be equal to the dissociation rate of the bound DABCO from the zinc center of the 1:1 DABCO–**Zn-1** complex, and cannot be accelerated by unbound DABCOs. Thus, the change in the chemical exchange is interpreted as a combination of these two mechanisms, that is, the associative guest-exchange becomes dominant over the dissociative mechanism when the amount of DABCO exceeds 1 equiv. As shown in Figure 3, the rapid chemical exchange between the peaks for C and D already started in the presence of 1 equiv of DABCO, which cannot be explained only by the dissociative mechanism. At this point, the concentration of unbound DABCO is calculated to be ca. 19 μM. This illustrates how effectively the unbound DABCO can accelerate the chemical exchange of species A and B.

In summary, DABCO undergoes a rapid exchange between the two binding pockets of the zinc porphyrin receptor **Zn-1** when more than 1 equiv of DABCO is added. The dissociation of DABCO is facilitated by binding of another molecule of DABCO to the opposite face of the zinc porphyrin receptor. This phenomenon should be general for the complexation of amine guests to zinc porphyrin receptors. Therefore, this new finding could provide valuable insight into understanding the stability of supramolecular porphyrin or related systems utilizing amine coordination as an organizing tool.[10]

This research was supported through a Grant-in-Aid for Scientific Research (No. 17750156 to Y.H.) from the Ministry of Education, Culture, Sports, Science and Technology Japan. We are grateful to T. Mizutani for valuable discussion, and to S. Kitagawa, H. Chang, and M. Higuchi for kind access and assistance to X-ray crystallography analysis.

## Supporting Information

Crystal structural data, ROE spectrum, and synthetic procedure of **Zn-1** and experimental details of NMR and UV–vis titration experiments. This material is available free of charge on the web at http://www.csj.jp/journals/bcsj/.

## References

1 H. Ogoshi, Y. Mizutani, T. Hayashi, Y. Kuroda, in *The Porphyrin Handbook*, ed. by K. M. Kadish, K. M. Smith, R. Guilard, Academic Press, San Diego, **2000**, Vol. 6, pp. 279–346, and references therein.

2 For a recent review, see: J. Weiss, *J. Inclusion Phenom. Macrocyclic Chem.* **2001**, *40*, 1, and references therein.

3 V. Heitz, J.-C. Chambron, J.-P. Sauvage, in *The Porphyrin Handbook*, ed. by K. M. Kadish, K. M. Smith, R. Guilard, Academic Press, San Diego, **2000**, Vol. 6, pp. 1–41, and references therein; B. G. Maiya, *J. Porphyrins Phthalocyanines* **2004**, *8*, 1118; A. Satake, Y. Kobuke, *Tetrahedron* **2005**, *61*, 13.

4 C. A. Hunter, M. N. Meah, J. K. M. Sanders, *J. Am. Chem. Soc.* **1990**, *112*, 5773; H. L. Anderson, C. A. Hunter, M. N. Meah, J. K. M. Sanders, *J. Am. Chem. Soc.* **1990**, *112*, 5780; T. Mizutani, T. Murakami, H. Ogoshi, *Tetrahedron Lett.* **1996**, *37*, 5369; V. V. Borovkov, J. M. Lintuluoto, H. Sugeta, M. Fujiki, R. Arakawa, Y. Inoue, *J. Am. Chem. Soc.* **2002**, *124*, 2993.

5 J. S. Lindsey, R. W. Wagner, *J. Org. Chem.* **1989**, *54*, 828; K. Tamao, K. Sumitani, Y. Kiso, M. Zembayashi, A. Fujioka, S. Kodama, I. Nakajima, A. Minato, M. Kumada, *Bull. Chem. Soc. Jpn.* **1976**, *49*, 1958; A. Iwasaki, Y. Kondo, K. Maruoka, *J. Am. Chem. Soc.* **2000**, *122*, 10238.

6 The ratio of the atropisomers was determined from the integrated area of $^1$H signals of the pyrrole $\beta$-protons of each atropisomer.

7 R. Song, A. Robert, J. Bernadou, B. Meunier, *Analusis* **1999**, *27*, 464; T. Hayashi, T. Asai, H. Hokazono, H. Ogoshi, *J. Am. Chem. Soc.* **1993**, *115*, 12210.

8 Crystallographic data have been deposited with Cambridge Crystallographic Data Centre: Deposition number CCDC-775279 for **Zn-1**. Copies of the data can be obtained free of charge via http://www.ccdc.cam.ac.uk/conts/retrieving.html (or from the Cambridge Crystallographic Data Centre, 12, Union Road, Cambridge, CB2 1EZ, UK; Fax: +44 1223 336033; e-mail: deposit@ccdc.cam.ac.uk).

9 For recent examples, see: J.-Q. Wang, C.-X. Ren, L.-H. Weng, G.-X. Jin, *Chem. Commun.* **2006**, 162; A. W. Kleij, M. Kuil, D. M. Tooke, A. L. Spek, J. N. H. Reek, *Inorg. Chem.* **2005**, *44*, 7696; D. J. Ring, M. C. Aragoni, N. R. Champness, C. Wilson, *CrystEngComm* **2005**, *7*, 621; E. Deiters, V. Bulach, M. W. Hosseini, *Chem. Commun.* **2005**, 3906; M. Vinodu, I. Goldberg, *New J. Chem.* **2004**, *28*, 1250.

10 K. Tashiro, Y. Hirabayashi, T. Aida, K. Saigo, K. Fujiwara, K. Komatsu, S. Sakamoto, K. Yamaguchi, *J. Am. Chem. Soc.* **2002**, *124*, 12086; T. Mizutani, S. Yagi, A. Honmaru, T. Goldacker, S. Kitagawa, M. Furusyo, T. Takagishi, H. Ogoshi, *Supramol. Chem.* **1999**, *10*, 297.